Prediction of Mine Gas Content Using Optimized Backpropagation Neural Networks and Genetic Algorithms for Fire Prevention

Yongming Zou[1, 2, 3]
[1]China Coal Research Institute, Beijing 100013, China
[2]Shenyang Research Institute, China Coal Technology and Engineering Group, Shenfu Demonstration Zone, 113122, China
[3]State Key Laboratory of Coal Mine Disaster Prevention and Control, Shenfu Demonstration Zone, 113122, China
Email: Z7766618@126.com

Keywords: back propagation, genetic algorithm, gas, mine, fire extinguishing

Received: May 31, 2024

As one of the important causes of mine fires, predicting the distribution of gas content in mines is of great value. In order to predict the gas content in mines, a method combining Back Propagation (BP) network and Genetic Algorithm (GA) is proposed. This algorithm is used to optimize the structure and weight of BP neural network. It updates the network weights of BP by crossing and mutating, making it more adaptable and avoiding local extreme values. The results showed that the prediction error of BP-GA was about 0.5%, and the maximum error was 0.6%, which was lower than that of single BP and GA. In addition, the predicted value of the BP-GA was closer to the actual value, with a margin of error of 17.62 m³/t. In the mine gas prediction system, the BP-GA showed high accuracy. The prediction error range was 7.62 m³/t to 28.46 m³/t, the data transmission rate was between 80-89 Mbps, the response time was 180 ms-270 ms, and the fast data transmission was realized. Therefore, the system proposed in the study can stably predict the gas content in mines.

Povzetek: V članku je opisana povezava povratne propagacije in genetskega algoritma za napoved vsebnosti plinov v rudnikih v smislu ocene nevarnosti požara. Nova metoda izboljšuje stabilnost in prilagodljivost ter povečuje varnost pri preprečevanju požarov.

1 Introduction

Due to China's high demand for coal resources, a large number of mining operations will occur. However, mining is a high-risk job, with a closed mine environment and poor air quality, which can easily lead to accidents that threaten the safety of workers. Gas is harmful and explosive, posing significant health risks. Moreover, the high content of gas can easily cause explosions and fires in mines, leading to mine collapse. Therefore, predicting the gas content in mines has important value [1]. The traditional prediction of gas content in mines adopts two methods: constructing mathematical models and empirical prediction. The mathematical models generally use qualitative comparison methods and linear analysis methods to predict gas content by evaluating geological conditions, with low prediction accuracy. The empirical prediction method has strong subjectivity [2]. Therefore, this study proposes a new method for predicting the gas content in mines. The study proposes a combination of Back Propagation (BP) network and Genetic Algorithm (GA) to predict gas content by analyzing factors that affect gas content in mines. Both BP neural networks and GA have strong data analysis capabilities and strong inclusiveness for multi-source data processing. However, a single BP is prone to falling into local extrema, and the GA convergence is unstable. Therefore, the GA is used to optimize the structure of the BP neural networks to improve its predictive performance [3]. Then apply the optimized algorithm to the system to achieve the actual prediction function of the algorithm. In order to meet the above research content, the article is divided into five parts. The first part is the introduction of the research direction and content of the article. The second part is a literature review, summarizing the current research status of BP neural networks, GAs, and gas prediction in mines used in the study. The third part is the research method, which includes two sections. The first section is the basic principles of GA and BP neural network. The second section is their optimization process and system design research. The fourth part is the result analysis. The result analysis is divided into three sections. First, the data are preprocessed, then BP-GA performance is analyzed, and finally, the application effect of the prediction system under the algorithm is analyzed. Finally, there is a summary of the article, summarizing the research results and development.

2 Related works

BP is a back propagation neural network that utilizes error feedback. The network structure is divided into multiple layers and has high data processing capabilities, making it widely used in different fields. In ocean warning, Wang et al. used a MEA-BP hybrid strategy to predict wave heights. This method combined the local

search ability of BP and the global search ability of MEA, reducing the probability of improper convergence of the algorithm. Results showed that the hybrid strategy had high accuracy in predicting wave height [4]. Due to the impact of ultra-short-term solar radiation on the accuracy of photovoltaic power generation prediction, Hu et al. constructed a cloud movement prediction method using BP and GA. After training with a large amount of data, the method could achieve a prediction accuracy of 96% and could be suitable for cloudy climate environments [5]. Wan et al. proposed using a BP neural network to predict the oxygen concentration and temperature of coal powder in order to explore methods for suppressing coal powder spontaneous combustion and constructed a prediction model for coal powder low-temperature oxidation. The experimental results indicated that this method could achieve a good degree of fitting and complete the prediction [6].

The GA is an algorithm that simulates the evolution process of biological genes and chromosomes. It can achieve random search of data and search for the optimal solution based on similar natural elimination rules. This algorithm has high adaptability and therefore has a wide range of application value. Sun et al. improved the BP neural network using GA and constructed a prediction model for road surface skid resistance. The model first input asphalt pavement data in 3D format, then used a pendulum friction tester to obtain the friction coefficient of the pavement, and finally processed the data. Results showed that the prediction error of this algorithm was 12.1%, and it had high accuracy in this field [7]. Yang et al. designed a variable spacing array method using GA, which could compress the channel and cost of phased arrays and had strong global computing power. Results showed that this method could reduce the grating split level below -15.9 dB in a phased array with 52 sub arrays [8]. Cao et al. conducted an analysis of the fluid flow in a 600 kW asynchronous traction motor based on fluid mechanics to investigate the heat dissipation problem. Based on the analysis results, a mathematical model based on the GA was constructed. Results indicated that it could predict motor temperature and obtain the optimal optimization method [9].

Due to the diversity of gas forms, high variability in physical and chemical properties, and the risk of flammability and explosion in some gases, predicting gases in different scenarios has certain practical significance. Moreover, gases have different properties, so they can also be used for technological development. To predict the production of shale gas, Wang and Jiang combined linear and nonlinear prediction models to predict the content of shale gas. This model used two improved algorithms, NMGM-ARIMA and ARIMA-ANN, to predict the shale gas content in Pennsylvania and Texas. Results showed that NMGM-ARIMA algorithm error was within 4.31%, while the error of NMGM-ARIMA was within 3.16% [10]. Wang et al. constructed an insulation diagnosis method using residual CNN based on the insulation properties of gases. Firstly, this method characterized target data domain features. Secondly, a domain adversarial training strategy was used to transfer features and achieve adaptation between features and labels. Finally, the gradient convergence of the algorithm was accelerated. Results showed that the diagnostic accuracy of insulation defects using this method was 99.15% [11]. Chen et al. built an experimental platform and improved core experiments to predict the recovery rate of ultra-deep carbonate gas. The improved experiment included three representative pore network models and visualized the gas flow state in the pores. Results showed that the predicted recovery rate of this method was 72.24% [12]. Table 1 summarizes the research work.

Table 1: Summarizes the research work.

Year	Authors	Research Method	Advantages	Disadvantages
2018	Wang et al. [4]	BP neural network optimized by mind evolutionary algorithm	High accuracy in predicting ocean wave heights	Limited to ocean wave height prediction
2022	Hu et al. [5]	BP neural network and GA for cloud motion prediction	96% prediction accuracy in cloudy weather conditions	May not be applicable to non-cloudy conditions
2020	Wan et al. [6]	BP neural network for coal powder oxidation prediction	High fitting degree for predicting coal powder oxidation	Limited to coal powder oxidation scenarios
2021	Sun et al. [7]	GA improved neural network for asphalt pavement friction coefficient prediction	12.1% prediction error, high accuracy	Specific to asphalt pavement friction coefficient
2022	Yang et al. [8]	GA for sub-array grating lobe suppression	Strong global computing ability, reduced grating lobe level	Limited to sub-array grating lobe suppression
2023	Cao et al. [9]	GA for optimization of stator ventilation structure of traction motor	Effective temperature prediction and optimization methods	Specific to high-speed rail traction motors
2019	Wang and Jiang [10]	Linear and nonlinear prediction techniques with NMGM-ARIMA and ARIMA-ANN	Low prediction error (4.31% and 3.16%)	Focused on specific regions (Pennsylvania and Texas)

2021	Wang et al. [11]	Residual CNN for insulation diagnosis	99.15% accuracy in insulation defect diagnosis	Limited to insulation diagnosis
2021	Chen et al. [12]	Experimental platform and core experiments for gas recovery rate prediction	72.24% gas recovery prediction accuracy	Focused on ultra-deep carbonate gas reservoirs

In summary, BP neural networks and GA, as advanced intelligent algorithms, have been widely applied with different functions. At the same time, there is already some research combining the two and conducting experiments. The prediction of gas mainly focuses on the prediction of gas mining output with economic value, but the research on the prediction of gas content that threatens safety is rare. Therefore, this study proposes to use a combined BP neural network and GA to predict the gas content in mines, aiming to reduce the risk of mine fires caused by gas explosions.

3 Improved BP-GA application in mine gas prediction

Due to the high risk of fire accidents when the gas content reaches a certain concentration, gas has always been an important cause of mine fires. In order to effectively reduce the risk of mine fire accidents caused by gas, this study proposes to construct a gas prediction model using BP and GA and apply it to the system to achieve intelligent gas content prediction. This section includes two sections. The first section introduces the construction of the BP-GA prediction model. The second section is the research on system design under the predictive model.

3.1 Theoretical research on BP and GA

BP is a unidirectional artificial neural network model and one of the earliest neural networks applied to practical problems. Due to the fact that the BP neural network is a supervised learning algorithm, it is mainly used to solve problems such as classification and recognition prediction. The structure of this network consists of three layers, namely input, hidden, and output layers [13]. Among them, the input layer is activated using the sigmoid function, the hidden layer operates on the network weights as the main connection between nodes, and the hidden and output layers transmit data by introducing a linear function. Assuming that the input node is $X=\{x_1,x_2,...,x_n\}$, the hidden layer is m neurons, and the hidden layer node is y_i, the output nodes of the hidden layer can be obtained as shown in Equation (1).

$$y_i = f\left(\sum_j W_{ij}X_j - \theta_i\right) \tag{1}$$

In Equation (1), $f(*)$ is the sigmoid activation function. W_{ij} is the input weight. θ_i is the input node threshold. At the same time, there are different weights between nodes that are connected to the input and output layers, and the output value of the output layer is O_l. The expression of O_l is shown in Equation (2).

$$O_l = F\left(\sum_i T_{ij}y_j - \theta_l\right) \tag{2}$$

In Equation (2), $F(*)$ is a linear function. T_{ij} is the output weight. θ_l is the output node threshold. There is a close connection between BP neural networks for calculating input data, as shown in Figure 1.

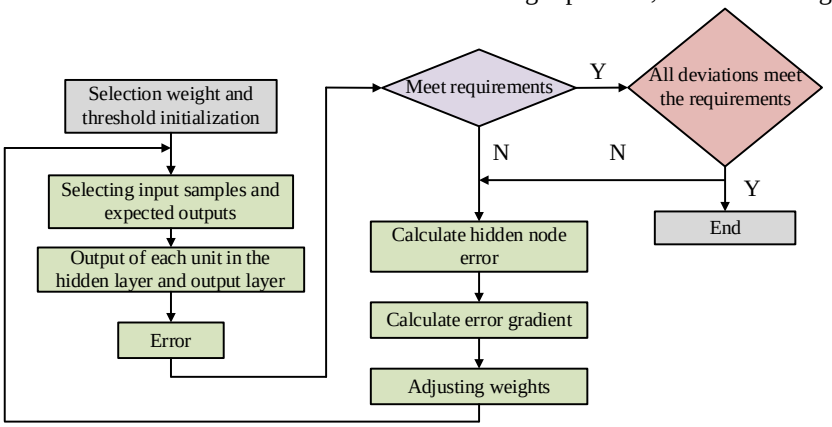

Figure 1: The BP operational flowchart.

Figure 1 shows the BP operational flowchart. Firstly, the BP initial learning frequency is set to $k=0$. Then natural numbers with smaller values are randomly selected to initialize the input weights and thresholds. The initialized parameter range is shown in Equation (3).

$$\begin{cases} W_{ij}(k)\in[-1,1] \\ T_{ij}(k)\in[-1,1] \\ \theta_i(k)\in[-1,1] \\ \theta_l(k)\in[-1,1] \end{cases} \tag{3}$$

In Equation (3), $W_{ij}(k)$, $T_{ij}(k)$, $\theta_i(k)$, and $\theta_l(k)$ are the initial input weight, output weight, input threshold, and output threshold, respectively. Given an input value of X and a target calculation value of P, then the results of the hidden layer and output layer in the network structure are calculated. The results of the hidden layer are shown in Equation (1), and the results of the output layer are shown in Equation (2). The error between the output result and the target value is calculated, and whether the error meets the preset value is determined. The formula for calculating the error value of the sample is shown in Equation (4).

$$e_k = \sum_{k=1}^{n}\sum_{l=1}^{n}\left|P^{(k)} - O_l^{(k)}\right| \tag{4}$$

In Equation (4), $P^{(k)}$ is the target output value and $O_l^{(k)}$ is the actual output value. e_k is the sample error value. If e_k satisfies the error within the operating range, the deviation is determined. If either deviation or error fails, it is necessary to calculate the parameter error during the calculation process, adjust the input value based on the results, and perform the calculation again until the calculation error requirements are met. The calculation formula for parameter error is shown in Equation (5).

$$\begin{cases} \delta_l = (P - o_l)\times o_l \times (1 - o_l) \\ T_{il}(k+1) = T_{il}(k) + \eta\delta_l y_i \\ \theta_l(k+1) = \theta_l(k) + \eta\delta_l \end{cases} \tag{5}$$

In Equation (5), δ_l, $T_{li}(k+1)$, and $\theta_l(k+1)$ are error modification values, weight errors, and threshold errors, respectively. η is the error parameter. o_l is the output node. BP neural network can modify samples by adjusting weights and thresholds. Although this method has high computational accuracy, its convergence speed is slow and it is easy to fall into local minima [14]. Therefore, in order to improve the performance of the algorithm and apply it to mine gas prediction, this study proposes the fusion of BP and GA to expand the algorithm's data parallel processing ability and fault tolerance ability. Because GA can compensate for BP local defects.

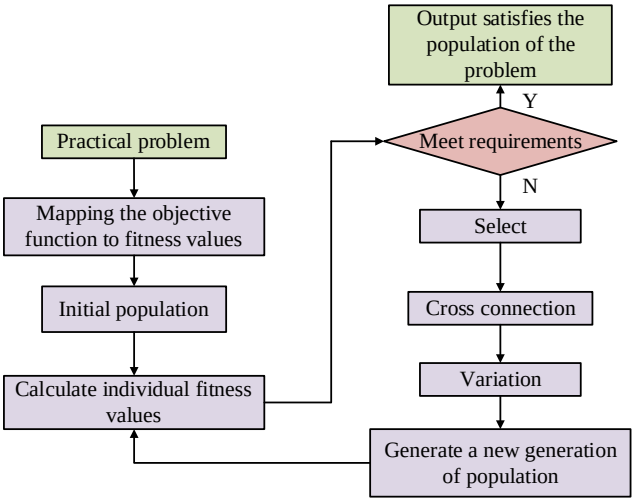

Figure 2: Operational flowchart of GA.

Figure 2 shows the GA operational flowchart. Firstly, convert the actual problem into different encoding forms, form the encoding into bit string form, and form the initial population. The operation of GA is essentially to construct a fitness function and calculate the fitness values of individual populations. Due to the algorithm selecting values with higher fitness values as genetic parents, the function values tend to be more inclined towards larger values. When the fitness value meets the requirements, the output population is the result. When the requirements are not met, it enters the core parts of GA, namely selection, crossover, and mutation [15]. Selection refers to using the proportional method to select the data with the highest fitness value as the parent, so the probability of an individual becoming a parent is directly proportional to the fitness value. The calculation of selection probability is shown in Equation (6).

$$P_{si} = \zeta_i / \sum_{j=1}^{M} f_i \tag{6}$$

In Equation (6), P_{si} is the probability that an individual is selected as the parent. ζ_i is the fitness value of the individual population. M is the population size. Crossing refers to the generation of new individuals that meet the characteristics of their parents by selecting individuals from two populations to cross. After completing the algorithm search through selection and crossover, mutation is used for global search. Until the individual search for the optimal fitness value is completed and a suitable population is output. A single GA has an immature convergence state, although it can perform global search. Therefore, the fusion of BP and GA can compensate for the shortcomings of the two

single algorithms, making the algorithm's adaptability more excellent.

3.2 Design and research of mine gas prediction system based on improved BP-GA

The study of 3.1 reveals that both single BP neural networks and GAs have inherent limitations. However, their respective advantages and disadvantages can be seen to complement each other. Therefore, integrating the two algorithms can improve the algorithm's global search ability and accurately select the optimal individual through error screening conditions.

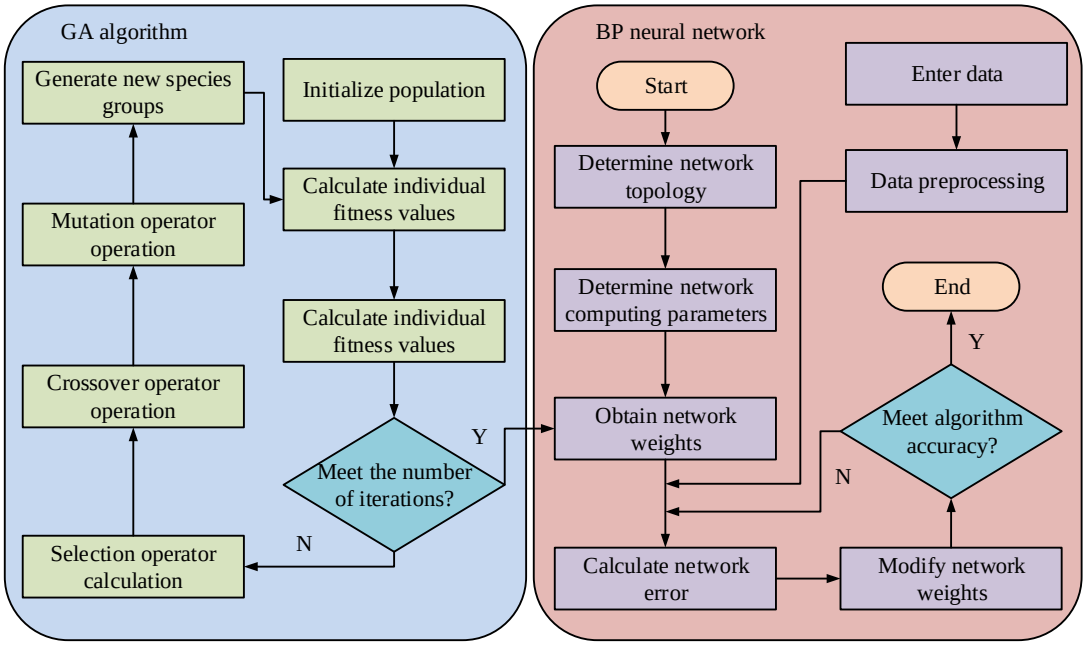

Figure 3: Improved operational flowchart for BP and GA.

Figure 3 shows the operational flowchart of the improved BP and GA. Firstly, an initial population $X=\{x_1,x_2,...,x_n\}$ is randomly generated based on existing individuals, where the ownership value of any x_i in X will form an individual. Then the individual is train and their fitness values are calculated. The fitness value expression at this point is shown in Equation (7).

$$\zeta_i=\frac{1}{\frac{1}{2}\sum_{p=1}^{m}\sum_{k=1}^{n}\left(V_{pk}-T_{pk}\right)} \tag{7}$$

In Equation (7), ζ_i is the fitness value of the individual i. m counts learning samples. V_{pk} is the output value of the k-th node of the T_{pk}-th individual. G is the expected output value. Then select the individual, and the selection probability can be calculated using Equation (6). Then perform individual crossover and mutation calculations for the improved algorithm, and the individual crossover rate p_c at this time is shown in Equation (8).

$$p_c=\begin{cases}p_{c1}-\dfrac{\left(p_{c1}-p_{c2}\right)\left(f^{'}-f_{\max}\right)}{f_{\max}-f_{avg}} \\ p_{c1},\ f\le f_{avg}\end{cases} \tag{8}$$

In Equation (8), f_{avg} and $f_{\max}$ are the average and maximum fitness values of the population, respectively. p_{c1} and p_{c2} are the individual's maximum and minimum crossover rates, respectively. f' is the maximum fitness value among crossover individuals. The formula for calculating the individual's mutation rate p_m is shown in Equation (9).

$$p_m=\begin{cases}p_{m1}-\dfrac{\left(p_{m1}-p_{m2}\right)\left(f_{\max}-f\right)}{f_{\max}-f_{avg}} \\ p_{m1},\ f\le f_{avg}\end{cases} \tag{9}$$

In Equation (9), p_{m1} and p_{m2} are the maximum and minimum individual variation rates, respectively. Then calculate the updated individual error and fitness values again. Moreover, globally search for the individual with the optimal fitness value. If the calculation range of the individual is within the expected range, output the result. Otherwise, recalculate the fitness value. Finally, the optimal individual output is decoded to obtain the optimal weight value, and then the input data is processed using the BP algorithm with it until the operation is completed [16].

The above content constructs a prediction model that improves the BP-GA. Applying this model to the actual prediction of mine gas is beneficial for reducing the

pressure of mine fire prevention and extinguishing. The process of monitoring the concentration of gas in coal mines is referred to as gas prediction. This monitoring allows for the accumulation of gas to be predicted, thus enabling the implementation of appropriate protective measures. According to the system design principles and network implementation, this study adopts the B/S system as the basic architecture. The system under this architecture is divided into a client front-end and a server back-end. The hardware architecture of the gas content prediction system is shown in Figure 4.

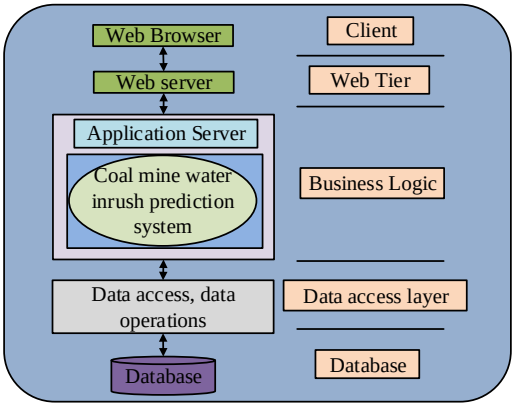

Figure 4: Hardware architecture of gas content prediction system.

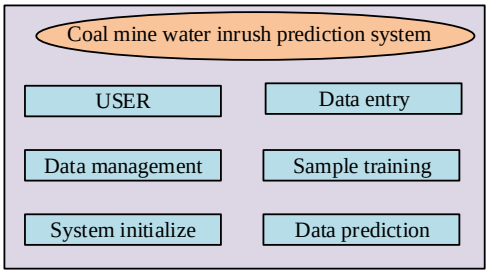

Figure 5: Structure diagram of gas prediction module.

Figure 4 shows the hardware architecture of the gas content prediction system. The client, as the starting end, sends task requirements, which are then executed through the web layer, business layer, data layer, and database to meet customer needs, and ultimately feedback the results to the client. Among them, the business layer is the core of executing task requirements, and the improved BP-GA is applied to the data prediction module in the business layer. The database contains all geological information in the mine and is monitored and managed by the system [17-19]. When the system performs prediction tasks, it needs to first input the actual conditions of the mine, including geological conditions, mining conditions, and structural conditions. Then select the trained improved BP-GA prediction model to process the data and use the model's mapping ability to predict the gas content in the mine. The specific prediction model structure is shown in Figure 5.

Figure 5 shows the structure diagram of the gas prediction module. Firstly, administrators can add user information and assign different permissions to users through the user management function. Then, a data table is established through the MySQL database for data management. Users can make changes to the data table to provide data for training the prediction model. Before entering the training module, it is necessary to initialize the data. After initialization, the default prediction model of the system is the optimization model, and the parameters cannot be changed [20]. The expression of the system initialization module is shown in Equation (10).

$$[w1, b1, w2, b2] = initff(P, S1, 'tansig', t, 'purelin') \tag{10}$$

In Equation (10), $w1$ and $b1$ represent the input layer connection weight and connection threshold, while $w2$ and $b2$ represent the hidden layer connection weight and threshold, respectively. $S1$ counts hidden layer neurons. P is the input data. $tansig$ and $purelin$ are tangent S-type functions and linear functions, respectively. After initialization, the model can be trained by inputting different parameter values. The data entry function enables modifications to the sample data necessary for training, input of data into the module controls, and subsequent programming of the data to be entered. This allows for training of the model based on the already entered data. Finally, in the prediction module, the trained model predicts the target sample data. Based on results, gas content in the mine is predicted to make

timely firefighting decisions.

4 Mine gas prediction algorithm and system application performance analysis based on improved BP-GA

In order to achieve intelligent prediction of mine gas content, a prediction model was designed by combining BP and GA, and the model was applied to a computer system. To verify the predictive performance and system application effectiveness of BP-GA, corresponding experiments were designed and analyzed in this section. SQL Server 2005 database, AMD Turion(tm) 64X2 mobile edition, 2GB central processor and Windows 2011 operating system are selected for the experiment. The BP neural network is configured as follows: the input layer is activated using the Sigmoid function and contains multiple input nodes. The output layer transmits data by introducing linear functions. The initial learning frequency is set to 0.03. Small natural numbers are randomly selected to initialize input weights and thresholds. The expected error is set at 0.001. The experiment modify the sample by adjusting the weights and thresholds. The training data set selects the actual data of a mine in China, with a sample size of 110, including 91 training data and 19 test data. The GA parameters are as follows: the population size is 150 and the maximum number of iterations is 250. The fitness function uses a formula to calculate the fitness value, and the data with the highest fitness value is used as the parent.

4.1 Data preprocessing

Data acquisition in mine environment may be affected by many factors, such as equipment error, environmental change, etc. These noises will affect the accuracy of prediction model. As the concentration of gas in mines is affected by a variety of complex factors, there may be systematic deviations in the collected data, such as geological conditions and mining methods. These are not adequately reflected in the data. Therefore, the normalization of data can reduce the difference between different data dimensions and improve the training effect of the model. The utilization of filtering technology serves to eliminate extraneous noise from data, thereby enhancing the overall quality of the data and, consequently, the precision of the model prediction. Due to the complex types of factors that affect gas content in the mine environment, there were significant dimensional differences. Therefore, data were normalized. The improved BP-GA in this study used the sigmoid function as the activation function. In order to normalize the input data, the input range can be set between (0,1), and all logical data can be expressed in the form of 0 or 1. Numerical data, on the other hand, adopted linear transformation to unify dimensions.

4.2 Performance analysis of improved BP-GA

The study fused BP and GA, trained the fused algorithm, and conducted performance comparison tests based on the results. The training dataset selected actual data from a certain mine in China, with a sample size of 110, 91 trained data, and 19 tested data. Simulation experiments were set up to analyze the performance of the algorithm, with a learning rate of 0.03 and an expected error of 0.001. The number of sample training sessions was divided into 4000 and 8000. Performance analysis was performed using a single BP neural network and GA as a comparison algorithm. The simulation experimental environment is shown in Table 2.

Table 2: Simulation experiment environment.

Experimental Platforms	Visio studio 2005
Experiment Language	C#
Database	SQL Server 2005
Hardware environment	AMD Turion(tm) 64 X2 Mobile
CPU	2GB
Operating System	Windows 2011

Table 2 shows the simulation experiment environment table. In the operation system of BP neural network, the selection of operators adopted proportion, with a population size of 150 and a maximum number of iterations of 250. The performance of the three algorithms was analyzed according to the above computing system and experimental environment to testify the performance of BP-GA.

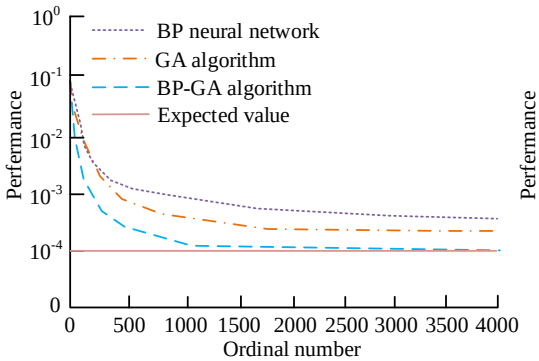

(a) Algorithm performance at 4000 training counts

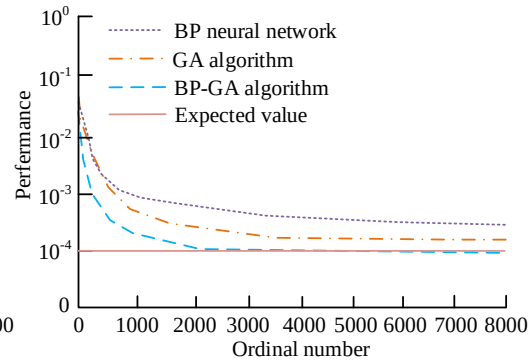

(b) Algorithm performance at 8000 training counts

Figure 6: Performance of different algorithms with different training sessions.

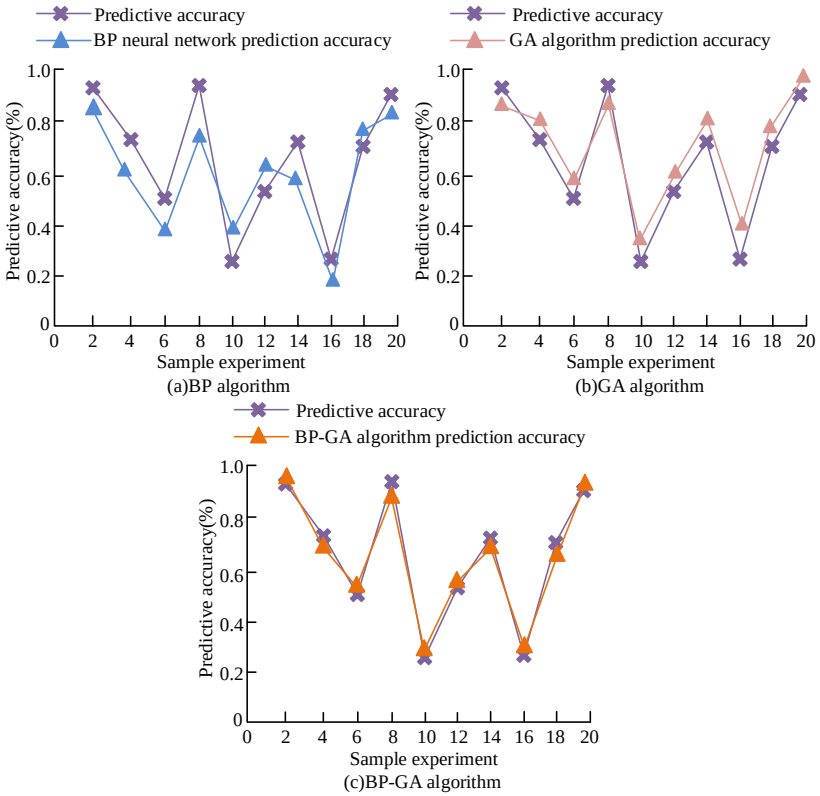

Figure 7: Prediction accuracy with different algorithms.

Figure 6 shows different algorithms performance under different training times. Among them, Figures 6 (a) and (b) show the algorithm performance under 4000 and 8000 training cycles, respectively. It can be concluded that compared to training 4000 times, the algorithm performance at 8000 times was closer to the convergence value. This indicated that as training sessions increased, the algorithm performance became more stable. As the number of iterations increased, the BP-GA can gradually converge to a stable state, indicating that there was no interference from local extremum in BP-GA, which can make it more stable and reach the expected value.

Figures 7 (a), (b), and (c) show the prediction accuracy of BP, GA, and BP-GA, respectively. The error between the BP and GA and the expected prediction value was relatively large, as both algorithms had local search extremum, which affected the algorithm prediction accuracy. BP-GA can effectively avoid local extremum, thus making the prediction accuracy closer to the true value. Therefore, the BP-GA was more in line with the expected values.

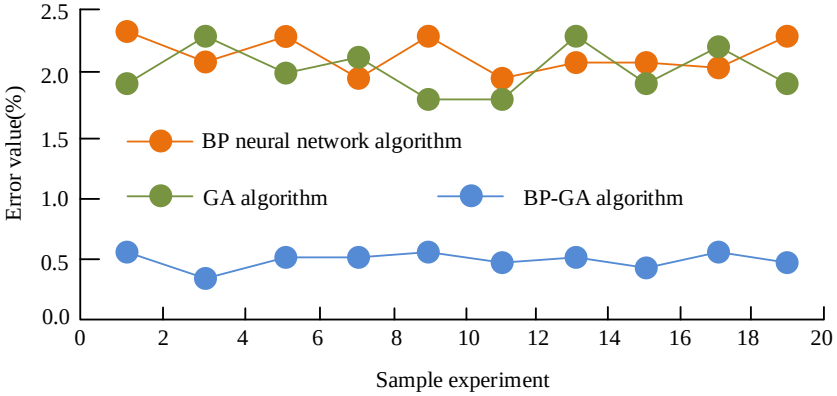

Figure 8: Test errors for different algorithms.

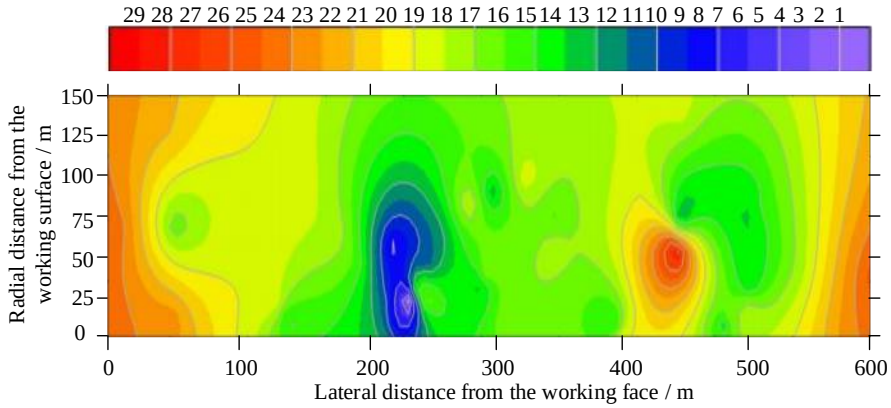

Figure 9: Three-dimensional map of mine gas content prediction.

Figure 8 shows the testing errors of different algorithms. The prediction error of the BP neural network was above 2.0%, with a maximum of 2.3%. That of the GA was also at a maximum of 2.3%, while that of BP-GA was around 0.5%, with a maximum of only 0.6%. BP-GA can use the global search of GA to avoid local minimum values in BP algorithm, and can also achieve complete and stable convergence. Therefore, this algorithm had stronger adaptability and can make the prediction results within a certain low error range.

4.3 Performance analysis of mine prediction system based on BP-GA

The training of the model was completed according to 4.2 and apply the trained prediction model to the mine gas content prediction system. An area with a radial length of 600 m and a lateral length of 150 m were selected as the prediction area in the mine, and 30 points were selected as experimental prediction points in the prediction area. The real-time data of the detected prediction points were input into the system and gas content prediction was performed on them.

Figure 9 shows a three-dimensional prediction of mine gas content. The gas content in the blue purple area in the figure was the lowest. Moreover, as it extended towards the surrounding environment, the gas content gradually increased. In the yellow green area, the gas content was in a transitional state from low to high, ultimately forming a range circle with high gas concentration. In the range of radial length from 410 m to 450 m and lateral length from 40 m to 60 m, the gas content was the highest, with an overall gas content range of approximately 21.02 $m^3 \cdot t^{-1}$-28.46 $m^3 \cdot t^{-1}$. The overall gas content of the mine detection points is shown in Table 3.

Table 3 shows the gas content values at the detection points of the mine. The predicted gas content at 30 detection points showed significant differences. Within the range of detected mines, the content of gas varied from 7.627.62 $m^3 \cdot t^{-1}$ to 28.467.62 $m^3 \cdot t^{-1}$. The predicted gas content values at different detection points were close to the true values, with an error range of around 17.62 $m^3 \cdot t^{-1}$. The implementation of multiple detection points in the system was beneficial for technical personnel to promptly identify risk points or triggering points during protection or accident analysis. Therefore, using the BP-GA prediction system to predict the gas content in mines had high accuracy and practical application value.

Table 3: Gas content data of mine testing points.

Serial number	Predicted value ($m^3 \cdot t^{-1}$)	Real value	Serial number	Predicted value ($m^3 \cdot t^{-1}$)	Real value
1	23.56	23.62	16	26.62	26.45
2	24.66	24.48	17	18.68	18.23
3	21.65	21.3	18	21.49	21.02
4	16.79	16.51	19	26.68	26.13
5	15.34	15.12	20	25.68	25.01
6	22.42	22.01	21	28.46	28.38
7	13.14	13.62	22	25.14	24.68
8	9.87	9.72	23	23.16	22.69
9	7.62	7.51	24	19.57	19.19
10	21.95	21.43	25	15.31	15.95
11	20.79	20.42	26	14.27	14.16
12	19.58	19.13	27	13.64	13.97
13	17.46	17.14	28	20.16	20.35

14	18.59	18.26	29	21.84	21.02
15	14.06	14.95	30	22.39	21.68

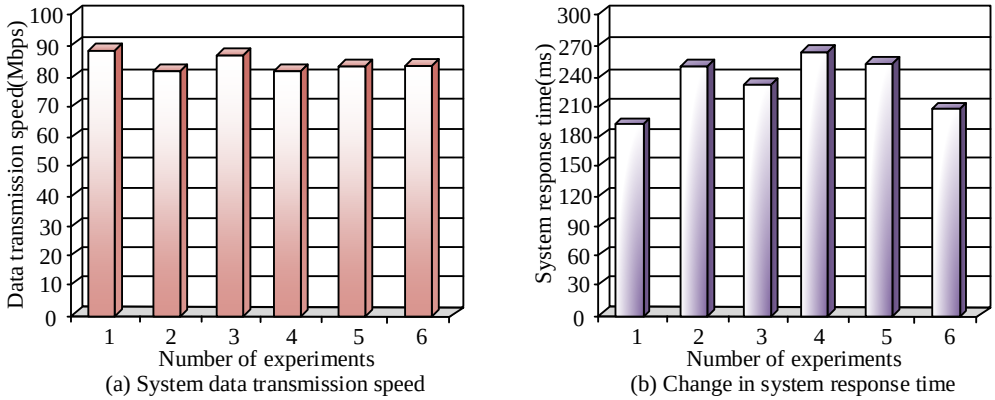

(a) System data transmission speed (b) Change in system response time

Figure 10: Performance diagram of BP-GA gas prediction system.

Table 4: Performance comparison results of each prediction algorithm on three data sets.

Method		SQL Server 2005 database	Kaggle data set	UCI machine Learning Library
Research method	Accuracy	0.92	0.91	0.89
	AUC value	0.95	0.91	0.90
Literature [4]	Accuracy	0.87	0.88	0.85
	AUC value	0.89	0.86	0.83
Literature [5]	Accuracy	0.89	0.86	0.82
	AUC value	0.90	0.84	0.82
Literature [7]	Accuracy	0.90	0.89	0.88
	AUC value	0.91	0.86	0.81

Figure 10 shows the performance diagram of the BP-GA gas prediction system. Among them, Figures 10 (a) and (b) show the data transmission rate and response time performance of the system, respectively. In six parallel experiments, the data transmission efficiency of the system remained stable between 80-89 Mbps, and the response time ranged from 180 ms to 270 ms. This indicated that the prediction system can achieve fast data transmission efficiency in a relatively short time. Therefore, the research and design of the BP-GA system had certain practical application value. The prediction accuracy, and AUC value of the proposed BP-GA prediction method were compared with those in the literatures [4], [5], [7] on different data sets. The results are shown in Table 4.

Table 4 shows that the accuracy of the research method in SQL Server 2005 database is 0.92, and the AUC value was 0.95. The accuracy and AUC values of the Kaggle dataset were both 0.91. The UCI machine learning library had an accuracy of 0.89 and an AUC value of 0.90. In contrast, the algorithms in literature [4], [5] and [7] performed poorly. The research method performed better than the literature method on all data sets. Especially on the AUC value, it showed its advantages in recognition accuracy and stability, indicating that it has strong generalization ability and robustness. Moreover, it is suitable for different data sets and application scenarios.

5 Discussion

Wang et al. [4] combined the local search capability of BP and the global search capability of MEA. It used the MEA-BP hybrid strategy to predict the wave height, reducing the probability of improper convergence of the algorithm. Using BP and GAs, Hu et al. [5] proposed a cloud motion prediction method with a prediction accuracy of 96%, which was suitable for cloudy climates. Wan et al. [6] used BP neural network to predict oxygen concentration and temperature of pulverized coal. The study built a prediction model for low-temperature oxidation of pulverized coal, and the results showed a good fit. Sun et al. [7] improved BP neural network by GA to build a prediction model of pavement skid resistance with a prediction error of 12.1%. After 8000 training, the prediction error of the research algorithm was stable at about 0.5%, showing high accuracy and effectively avoiding the limitations of a single algorithm. The error of the improved BP-GA in predicting mine gas content was significantly reduced (the maximum error was only 0.6%), while the error of the traditional BP or GA was larger (the maximum error was 2.3%). In general, the performance of the hybrid algorithm combining BP and GA was better than that of the single algorithm in various fields, especially in the prediction accuracy and convergence stability.

6 Conclusion

As one of the important energy sources, coal has been extensively exploited in many countries. However, high concentrations of gas are easily accumulated in mines generated by coal mining. Gas is flammable and explosive gas, which threats workers safety in enclosed my spaces. Therefore, predicting the gas content in mines has high research significance. This study was proposed to optimize BP using GA, input it into GA, calculated the network weight of BP structure through the cross-mutation operation of GA, and updated it. The updated BP structure performed operational analysis on the normalized preprocessed data, in order to input the operational results and complete data prediction. The experimental results showed that the BP optimized by GA achieved stable performance after training 8000 times, and the prediction error was only about 0.5%. By predicting the experimental mine, it could be concluded that the gas content range of the mine was between 7.62 $m^3 \cdot t^{-1}$ and 28.46 $m^3 \cdot t^{-1}$. The data transmission efficiency of the system using this algorithm was between 80-89 Mbps, and the response time was within the range of 180 ms-270 ms. Therefore, the algorithm proposed in the study not only has stable performance, but also can achieve efficient system application effects. Further research can be conducted on the universality of prediction systems by expanding the types of mines in the future.

References

[1] Hee-Sung Bae, Laibin Huang, John R. White, Jim Wang, Ronald D. DeLaune, and Andrew Ogram. Response of microbial populations regulating nutrient biogeochemical cycles to oiling of coastal saltmarshes from the deepwater horizon oil spill. Environmental pollution, 241: 136-147, 2018. https://doi.org/10.1016/j.envpol.2018.05.033

[2] Michael Bock, Hilary Robinson, Richard Wenning, Deborah French-McCay, Jill Rowe, and Ann Hayward Walker. Comparative risk assessment of oil spill response options for a deepwater oil well blowout: Part II. Relative risk methodology. Marine pollution bulletin, 2018, 133: 984-1000, 2018. https://doi.org/10.1016/j.marpolbul.2018.05.032

[3] Xiaolei Cai, Jiaqing Chen, Yipeng Ji, Meili Liu, and Wenjin Liu. Structural optimization and performance prediction of a compact flotation unit using GA-BP neural network with computational fluid dynamics simulation. Environmental engineering science, 36(9): 1185-1198, 2019. https://doi.org/10.1089/ees.2018.0327

[4] Wenxu Wang, Ruichun Tang, Cheng Li, Peishun Liu, and Liang Luo. A BP neural network model optimized by mind evolutionary algorithm for predicting the ocean wave heights. Ocean Engineering, 162: 98-107, 2018. https://doi.org/10.1016/j.oceaneng.2018.04.039

[5] Keyong Hu, Lidong Wang, Wenjuan Li, Shihua Cao, and Yuyan Shen. Forecasting of solar radiation in photovoltaic power station based on ground-based cloud images and BP neural network. IET Generation, Transmission & Distribution, 16(2): 333-350, 2022. https://doi.org/10.1049/gtd2.12309

[6] Yongzhou Wan, Jiaxin Wu, Ruizhi Chu, Zhenyong Miao, Lulu Fan, Lei Bai, and Xianliang Meng. Prediction of BP neural network and preliminary application for suppression of low-temperature oxidation of coal stockpiles by pulverized coal covering. The Canadian Journal of Chemical Engineering, 98(12): 2587-2598, 2020. https://doi.org/10.1002/cjce.23860

[7] Zhaoyun Sun, Xueli Hao, Wei Li, Ju Huyan, and Hongchao Sun. Asphalt pavement friction coefficient prediction method based on genetic-algorithm-improved neural network (GAI-NN) model. Canadian Journal of Civil Engineering, 49(1): 109-120, 2021. https://doi.org/10.1139/cjce-2020-0051

[8] Lei Yang, Kan Wang, and Hongbing Sun. A grating lobe suppression method for displaced subarrays using genetic algorithm. IET Microwaves, Antennas & Propagation, 16(7): 457-464, 2022. https://doi.org/10.1049/mia2.12258

[9] Cao Junci, Yan Hua, Li Wenlong, Li Dong, and Wang Yu. Optimization of stator ventilation structure of high-speed railway traction motor based on the genetic algorithm. IET Electric Power Applications, 17(3): 281-292, 2023. https://doi.org/10.1049/elp2.12263

[10] Qiang Wang, and Feng Jiang. Integrating linear and nonlinear forecasting techniques based on grey theory and artificial intelligence to forecast shale gas monthly production in Pennsylvania and Texas of the United States. Energy, 178(6): 781-803, 2019. https://doi.org/ 10.1016/j.energy.2019.04.115

[11] Yanxin Wang, Jing Yan, Qianzhen Jing, Zhenkang Qi, Jianhua Wang, and Yingsan Geng. A novel adversarial transfer learning in deep convolutional neural network for intelligent diagnosis of gas-insulated switchgear insulation defect. IET Generation, Transmission & Distribution, 2021, 15(23): 3229-3241, 2021. https://doi.org/10.1049/gtd2.12255

[12] Jianxun Chen, Shenglai Yang, Qingyan Mei, Jingyuan Chen, Hao Chen, Cheng Zou, Jiajun Li, and Shan Yang. Influence of pore structure on gas flow and recovery in ultradeep carbonate gas reservoirs at multiple scales. Energy & Fuels, 2021, 35(5): 3951-3971, 2021. https://doi.org/10.1021/acs.energyfuels.0c04178

[13] Jinyu An, and Shini Peng. Prediction and verification of risk loss cost for improved natural gas network layout optimization. Energy, 148(5): 1181-1190, 2018. https://doi.org/10.1016/j.energy.2018.01.143

[14] E. M. Arun Sankar, Mohammad Shahab, and Raghunathan Rengaswamy. Spacing optimization for active droplet sorting in microfluidic networks using genetic algorithm. Industrial & Engineering Chemistry Research, 60(4): 1699-1708, 2021. https://doi.org/10.1021/acs.iecr.0c04455

[15] K. Lactis, hIFN-γ, substrate inhibition, Box-Behnken, and ANN-GA. Artificial neural network-genetic algorithm (ANN-GA) based medium optimization for the production of human interferon gamma (hIFN-γ) in Kluyveromyces lactis cell factory. The Canadian Journal of Chemical Engineering, 97(4): 843-858, 2019. https://doi.org/ 10.1002/cjce.23350

[16] Khan Ammara Anjum, Abolhasan Mehran, Ni Wei, Lipman Justin, and Jamalipour Abbas. A hybrid-fuzzy logic guided genetic algorithm (H-FLGA) approach for resource optimization in 5G VANETs. IEEE Transactions on Vehicular Technology, 68(7): 6964-6974, 2019. https://doi.org/10.1109/TVT.2019.2915194

[17] Nelson J. R. Fagundes, Nicolas Ray, Mark Beaumont, Samuel Neuenschwander, Francisco M. Salzano, Sandro L. Bonatto, and Laurent Excoffier, Statistical evaluation of alternative models of human evolution. Proceedings of the National Academy of Sciences of the United States of America, 104(45): 17614-9, 2007. https://doi.org/10.1073/pnas.0708280104

[18] Yulong Yang, Tongjing Liu, Yanyue Li, Yuqi Li, Zhenjiang You, Mengting Zuo, Pengxiang Diwu, Rui Wang, Xing Zhang, and Jinhui Liang. Effects of velocity and permeability on tracer dispersion in porous media. Applied sciences, 11(10): 38-45, 2021. https://doi.org/10.3390/app11104411

[19] Maxime Martinasso, Miguel Gila, Mauro Bianco, Sadaf Alam, Colin McMurtrie, and Thomas C. Schulthess. RM-Replay: A High-Fidelity Tuning, Optimization and Exploration Tool for Resource Management. International Conference for High Performance Computing, 1: 320-332, 2018. https://doi.org/10.1109/SC.2018.00028

[20] Shahabadi Maziar Bani, Buehner Mark, Aparicio Josep, and Garand Louis. Implementation of slant-path radiative transfer in environment Canada's global deterministic weather prediction system. Monthly Weather Review, 148(10): 4231-4245, 2020. https://doi.org/10.1175/MWR-D-20-0060.1